



日本原子力研究開発機構機関リポジトリ
Japan Atomic Energy Agency Institutional Repository

Title	Analysis of the ozone reduction event over the southern tip of South America in November 2009
Author(s)	Akiyoshi Hideharu, Kadowaki Masanao, Nakamura Haruna, Sugita Takafumi, Hirooka Toshihiko, Harada Yayoi, Mizuno Akira
Citation	Journal of Geophysical Research; Atmospheres, 123(22),p.12523-12542
Text Version	出版社版のみ(学会への申請不要)
URL	https://jopss.jaea.go.jp/search/servlet/search?5064255
DOI	https://doi.org/10.1029/2017JD028096
Right	American Geophysical Union

RESEARCH ARTICLE

10.1029/2017JD028096

Key Points:

- The dynamical fields in the Southern Hemisphere associated with a low total ozone event at Rio Gallegos in November of 2009 were analyzed
- The 2009 event occurred due to polar vortex migration toward South America and blocking in the troposphere over the Pacific
- The total O₃ anomaly in November 2009 was one of the largest for 1979–2015 in association with a large negative geopotential height anomaly

Supporting Information:

- Supporting Information S1

Correspondence to:

H. Akiyoshi,
hakiyosi@nies.go.jp

Citation:

Akiyoshi, H., Kadowaki, M., Nakamura, H., Sugita, T., Hirooka, T., Harada, Y., & Mizuno, A. (2018). Analysis of the ozone reduction event over the southern tip of South America in November 2009. *Journal of Geophysical Research: Atmospheres*, 123, 12,523–12,542. <https://doi.org/10.1029/2017JD028096>

Received 21 NOV 2017

Accepted 19 OCT 2018

Accepted article online 29 OCT 2018

Published online 19 NOV 2018

Author Contributions:

Conceptualization: Hideharu Akiyoshi

Formal analysis: Hideharu Akiyoshi, Masanao Kadowaki, Haruna Nakamura, Toshihiko Hirooka, Yayoi Harada, Akira Mizuno

Funding acquisition: Hideharu Akiyoshi, Toshihiko Hirooka, Akira Mizuno

Investigation: Takafumi Sugita, Toshihiko Hirooka, Akira Mizuno

Methodology: Hideharu Akiyoshi, Takafumi Sugita, Toshihiko Hirooka






Supervision: Hideharu Akiyoshi, Akira Mizuno

Validation: Takafumi Sugita, Toshihiko Hirooka

Visualization: Masanao Kadowaki, Haruna Nakamura, Yayoi Harada

Writing - original draft: Hideharu Akiyoshi, Masanao Kadowaki

Analysis of the Ozone Reduction Event Over the Southern Tip of South America in November 2009

Hideharu Akiyoshi¹ , Masanao Kadowaki^{2,1}, Haruna Nakamura³, Takafumi Sugita¹ , Toshihiko Hirooka⁴ , Yayoi Harada⁵ , and Akira Mizuno⁶ 
¹National Institute for Environmental Studies, Tsukuba, Japan, ²Japan Atomic Energy Agency, Tōkai, Japan, ³Fujitsu FIP Corporation, Tokyo, Japan, ⁴Department of Earth and Planetary Sciences, Kyushu University, Fukuoka, Japan,

⁵Meteorological Research Institute, Tsukuba, Japan, ⁶Institute for Space-Earth Environmental Research, Nagoya University, Nagoya, Japan

Abstract A reduction of the total ozone over the southern tip of South America lasting 3 weeks occurred in November 2009. Analyses of the ERA-Interim reanalysis data and the total ozone observed by the Ozone Monitoring Instrument indicate that the total ozone reduction event was caused by a migration of the polar vortex toward the South American continent at the time of the vortex breakup. The vortex migration is associated with an enhanced wave flux from the troposphere at 120–150°W and 50–60°S to the west of the South American continent to the stratosphere over the southern part of the continent, which led to a large negative geopotential height anomaly in the lower stratosphere. In November, a blocking event was diagnosed from the 500-hPa geopotential height over the west of the South American continent. These results suggest a relation between the long-lasting reduction of the total ozone over the southern tip of South America and the blocking phenomenon in the troposphere of the Southern Hemisphere through wave propagation from the blocking region in 2009. Analysis of the total ozone anomaly for 50–60°S and 65–75°W over the southern tip of South America in November for 1979–2015 indicates that the negative ozone anomaly in November 2009 was one of the largest anomalies in this 37-year period and was associated with the large negative geopotential height anomaly in the lower stratosphere. Analyses of dynamical fields were also conducted for other years with large geopotential height anomalies.

1. Introduction

An Antarctic ozone hole has occurred every year over Antarctica in austral spring since the early 1980s. When the ozone hole developed, the ozone concentration at middle and high latitudes in the Southern Hemisphere was temporarily reduced. Kirchhoff et al. (1997) reported a dramatic total column ozone (hereafter, total ozone) reduction as low as about 200 Dobson units (DU) over Punta Arenas, Chile, for 4–5 days in October 1995. Pérez et al. (2000) reported short-term low-ozone events at Rio Grande, Carmen de Patagones, and San Luis in the South American continent in September 1996 and October 1997. These low-ozone events were associated with polar vortex elongation in September and October in the direction of the southern part of the South American continent with an eastward phase shift. Brinksma et al. (2002) reported short-term low-ozone events over New Zealand in September, October, and November 1997. These low-ozone events were associated with polar vortex elongation and distortion in September and October and ozone-depleted vortex remnant advection after the vortex breakup in the direction of New Zealand in November. The transit of low-ozone air masses due to the polar vortex elongation and ozone-depleted vortex remnant advection after the vortex breakup caused a reduction of the total ozone amount over several days, because the phase (the longitude) of the polar vortex elongation travels eastward in September and October and the small-scale ozone-depleted vortex remnant is diluted, diffusively and chemically, for a short period in November.

In contrast to these short-term reductions, low-ozone events over New Zealand or the southern part of the South American continent can also occur just before or during the Antarctic polar vortex breakup due to polar vortex migration with low-ozone air masses. Ajtic et al. (2003) discussed the advection of such a low-ozone air mass to New Zealand in December 1998. In the southern part of South America, low total ozone was observed for a long period, totaling 3 weeks, in November 2009. The ozone reduction and associated increase in ultraviolet radiation were measured by lidar and radiometers at the Network for the Detection of Atmospheric Composition Change station at Rio Gallegos (51.5°S, 69.3°W) in Argentina (Wolfram et al.,

2012). Although the lidar observations were not performed daily, partly due to bad weather conditions, they showed ozone concentration reductions at altitudes of 20–35 km on 13–14 November 2009 and 15–25 km on 22–23 November 2009. The serial occurrence of ozone reductions at different altitudes resulted in a 3-week reduction in the total ozone as reported by de Laat et al. (2010).

An irreversible advection of a low-ozone air mass, as the polar vortex undergoes breakup, is a critical factor in ozone reductions lasting several weeks over the southern tip of the South American continent. The migration of the polar vortex, accompanied by a low-ozone air mass, often occurs during the period of polar vortex breakup (Atkinson & Plumb, 1997). This may result in a long period of ozone reduction in the regions around Antarctica. The distortion and breakup of the polar vortex are largely caused by an increase in planetary wave activity in the stratosphere. Therefore, an analysis of the planetary wave activity in 2009 may lead to a better understanding of the deformation and migration of the vortex.

In this study, we analyze the geopotential height field and wave activity flux, as well as the total ozone distribution at 50–60°S when the polar vortex migrated toward the southern part of the South American continent in November 2009. The geopotential height field is decomposed into zonal wavenumbers 1 and 2, which are the dominant components in the Southern Hemisphere. We also show a relation between the long-term low total ozone event observed over the southern part of the South American continent and a blocking phenomenon in the troposphere of the Southern Hemisphere. This is associated with the planetary wave propagation from the troposphere to the stratosphere during a low-ozone event. The analysis of the geopotential height field and the total ozone distribution for November 2009 is extended to November in the years from 1979 to 2015 to consider the geopotential height anomalies and the total ozone for these 37 years, and it is found that the November 2009 event was one of the largest negative anomalies.

2. Data for Analysis

2.1. Meteorological Data

The European Centre for Medium-Range Weather Forecasts provides ERA-Interim reanalysis data for the period from 1 January 1979 to the present (Dee et al., 2011). In this study, we utilize the daily-mean ERA-Interim reanalysis data for the 37 years from 1979 to 2015. The horizontal resolution of these data is $1.5^\circ \times 1.5^\circ$ in latitude and longitude. The vertical range spans 37 pressure levels from 1 to 1,000 hPa.

2.2. Total Ozone Data

We use the daily total ozone data from the observations by the Total Ozone Mapping Spectrometer (TOMS) from 1979 to 2005 and the Ozone Monitoring Instrument (OMI) from 2006 to 2015. The TOMS data used are the “TOMS Nimbus-7 Total Column Ozone Daily L3 Global $1^\circ \times 1.25^\circ$ Lat/Lon Grid V008” and “TOMS Earth Probe Total Column Ozone Daily L3 Global $1^\circ \times 1.25^\circ$ Lat/Lon Grid V008.” The OMI data used are the “OMI/Aura Ozone (O3) DOAS Total Column L3 1 day $0.25^\circ \times 0.25^\circ$ V3.” The URLs for these data sets are provided in the Acknowledgements.

2.3. Data From a Nudged Chemistry-Climate Model Simulation

In this study, we also use the output from a nudged chemistry-climate model (nudged CCM) to discuss the ozone variation over Rio Gallegos. The CCM used for this study is the MIROC 3.2 CCM, which was used for a global simulation of the ozone, HCl, and ClO during the stratospheric sudden warming event in the Northern Hemisphere high latitudes in January 2010 (Akiyoshi et al., 2016). The model is a global spectral model with T42 horizontal resolution ($2.8^\circ \times 2.8^\circ$) and 34 vertical atmospheric layers above the surface. The top layer is located at an altitude of approximately 80 km (0.01 hPa). See Akiyoshi et al. (2016) for details.

The data from the nudged CCM simulation used for the analyses presented in sections 3 and 7.2 are from the REF-C1SD simulation, which is recommended by the Chemistry Climate Model Initiative (CCMI; Eyring et al., 2013; Morgenstern et al., 2017). This simulation is identical to the REF-C1 simulation, which is a simulation of the past climate and chemical constituent distribution forced by the observation data of ozone depleting substances (ODS) concentration, greenhouse gas (GHG) concentration, sea surface temperature, sea ice, quasi-biennial oscillation, volcanic aerosols, and solar radiation variation, except that the meteorological fields are nudged toward the observations. The zonal wind velocity, the meridional wind

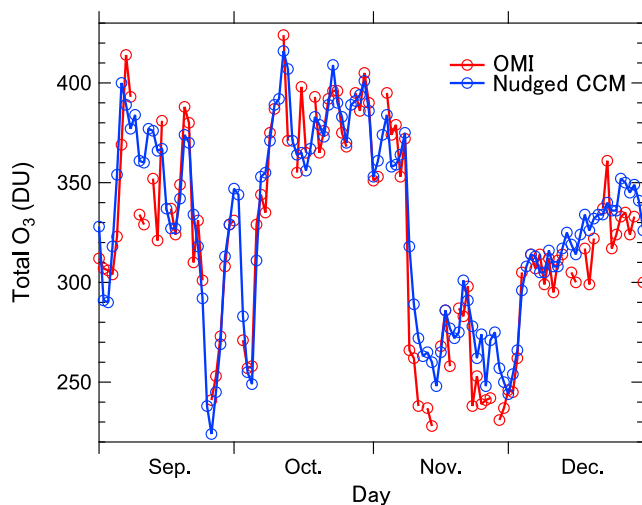


Figure 1. Time series of the total ozone over Rio Gallegos (51.5°S, 69.3°W) from 1 September to 31 December observed by the Ozone Monitoring Instrument (OMI; red) and calculated by the chemistry-climate model (CCM) nudged toward the horizontal winds and temperature of the ERA-Interim data (blue). DU = Dobson unit.

velocity, and the temperature in the CCM are nudged toward the daily data of the ERA-Interim reanalysis (Dee et al., 2011) below 1 hPa. Above 1 hPa, the zonal-mean zonal wind and temperature are nudged toward the zonal-mean monthly mean data of the COSPAR International Reference Atmosphere 86 (CIRA 1986; Rees et al., 1990). These daily and monthly data are linearly interpolated to the time steps of the CCM. The timescale for nudging of zonal winds, meridional winds, and temperature is set to 1 day.

3. Time Series of Observed and Simulated Total Ozone Over Rio Gallegos

At Rio Gallegos (51.5°S, 69.3°W) in the southern tip of South America, lidar measurements of the ozone profile were taken in spring 2009 (Wolfram et al., 2012), and a comparison among the lidar observations, the satellite observations by the Microwave Limb Sounder, and a nudged chemistry-climate model simulation from September to November was performed (Sugita et al., 2017). These observations and the model simulation demonstrated changes in the vertical profile of the ozone during the low-ozone event in November 2009. Figure 1 shows a comparison of the total ozone amounts over Rio Gallegos between TOMS/OMI and the nudged CCM from September to December 2009. The CCM reproduced very well the

observed total ozone amount and its variations over Rio Gallegos. At the end of September and the beginning of October, low-ozone events occurred over Rio Gallegos for several days. These events occurred when the tip of the elongated polar vortex passed over Rio Gallegos associated with the eastward traveling (rotation) of the vortex around the South Pole, as shown in Kirchhoff et al. (1997) and Pérez et al. (2000), while a low-ozone event lasting several weeks in November was associated with the polar vortex breakup process accompanied by polar vortex migration in the direction of the southern tip of the South American continent.

4. Migration of the Antarctic Polar Vortex Toward the South American Continent at the Time of Its Breakup in 2009

In middle to late November 2009, the Antarctic polar vortex gradually migrated toward South America and broke up in early to mid-December. According to the definition of Langematz and Kunze (2006), the breakup date was 4 December, when the zonal mean westerlies at 65°S at 50 hPa decreased below 10 m/s. Conversely, according to the definition of Wough and Rong (2002), the breakup date was 12 December, when the horizontal wind speed averaged along the vortex edge fell below the critical value of 15.2 m/s at the 500 K potential temperature surface. These two methods were used in Akiyoshi et al. (2009) to calculate the springtime breakup date of the Antarctic polar vortex. The vortex migration and breakup resulted in a long-lasting period of low total ozone over this region. Figure 2 shows the total ozone distribution observed by OMI and the potential vorticity distribution and polar vortex boundary calculated from the ERA-Interim reanalysis data in the Southern Hemisphere middle and high latitudes on 13 and 23 November 2009. The polar vortex boundary on Ertel's potential vorticity was calculated by the method of Nash et al. (1996). As shown in Figure 2, on 13 November, Rio Gallegos was inside the polar vortex as defined by the potential vorticity field at a potential temperature of 675 K and at the edge of the vortex at 475 K. By 23 November, Rio Gallegos was outside the polar vortex at 675 K due to a reduction in the vortex area at this altitude. Rio Gallegos remained inside the polar vortex at 475 K. The variations in the timings of the advection of vortex air at different altitudes over Rio Gallegos resulted in a 3-week total ozone reduction over the southern tip of South America, as shown in the time series of the total ozone over Rio Gallegos in Figure 1 and the total ozone map in Figures 2a and 2b. The average westerly zonal jet at the 675 K surface between 50°S and 75°S was 18.3 m/s on 13 November. This weakened to 10.3 m/s on 23 November. This indicates that the polar vortex at the upper altitudes had already begun to decay on 23 November. The polar vortex area at 675 K on 23 November in Figure 2 was reduced compared to its extent at 475 K on the same day and at 675 K on 13 November.

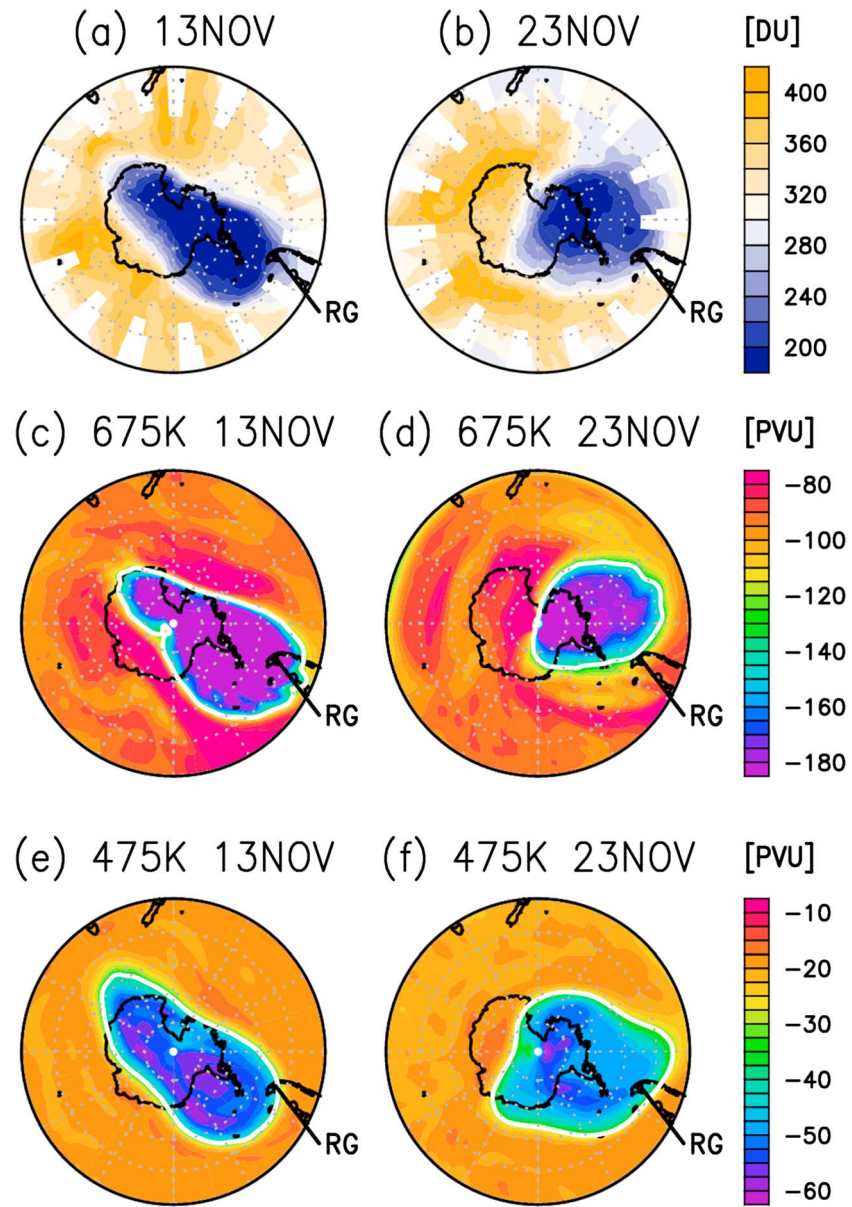


Figure 2. Total ozone distribution from the Ozone Monitoring Instrument in the Southern Hemisphere middle and high latitudes on 13 and 23 November 2009, and the potential vorticity distribution and polar vortex boundary on isentropic surfaces, derived from the ERA-Interim reanalysis data. Each projection corresponds to total ozone on 13 November (a) and that on 23 November (b), the potential vorticity at 675 K on 13 November (c) and that on 23 November (d), and the potential vorticity at 475 K on 13 November (e) and that on 23 November (f). The values for the total ozone are expressed in Dobson units ($1 \text{ DU} = 1 \text{ m-atm-cm} = 2.69 \times 10^{20} \text{ molecules/m}^2$), and those for the potential vorticity are expressed in potential vorticity units (PVU; $10^{-6} \text{ m}^2 \cdot \text{s}^{-1} \cdot \text{K} \cdot \text{kg}^{-1}$), indicated by color. The white area with rough boundaries in panels (a–b) indicates missing data. The boundaries of the polar vortex are indicated by thick solid white lines in panels (c–f). The outer boundary of each panel is 30°S. The location of Rio Gallegos is designated by the solid black triangle marked “RG.” The longitudes are bottom, 0°E; right, 90°W; top, 180°E; and left, 90°E.

5. Analysis of the Total Ozone and the Geopotential Height in November 2009

In this section, we compare the total ozone and the geopotential height in November 2009 with the climatology for the period 1979–2015. The geopotential height distribution, and thus the temperature distribution, is reflected in the total ozone distribution (Wirth, 1993).

Table 1

Correlation Coefficient Between the Total Ozone and the Geopotential Height at 50 hPa, 50–60°S and 69.3°W in November 1979–2015, Based on the Daily Data of Ozone Monitoring Instrument and ERA-Interim

Pressure (hPa)	Correlation coefficient
10	0.84
20	0.87
50	0.90
100	0.82
200	0.65

Note. The correlation coefficients are statistically significant at the 99.9% level according to a *t* test.

The South American continent is more vulnerable to low-column ozone in spring compared with Australia and New Zealand (Ajtic et al., 2004). A long-lasting low total ozone event over Rio Gallegos such as that in 2009 occurred with a dynamical field that was different from the climatology.

We investigate the wave components of the geopotential height at 50 hPa at the latitude range associated with this event. The choice of the 50-hPa level is based on the result of our analysis that the temporal correlation between the daily total ozone and daily geopotential height at 50–60°S and 69.3°W in November for the period 1979–2015 is highest at 50 hPa and has a positive value, as shown in Table 1. The correlations in the years 1979–1982, when the area of the ozone hole had not yet increased or had

just started increasing, are not as high as those after 1982, with values of 0.30, 0.48, 0.59, and 0.57 for the years 1979, 1980, 1981, and 1982, respectively. Note that the area of the ozone hole is defined by the area where the total ozone is less than 220 DU (e.g., NASA Ozone Watch, <https://ozonewatch.gsfc.nasa.gov/>). Although the spatial scale of the ozone-poor air mass is much smaller than that of the polar vortex, Iwao and Hirooka (2006) showed longitudinal positive correlations between the total ozone and geopotential height in the troposphere and stratosphere for the air mass originating from the ozone hole. Conversely, longitudinal negative correlations in the troposphere and weak correlations in the lower stratosphere were found for the air mass of the anticyclonic anomaly around the tropopause with tropopause uplift (see their Figures 14 and 12 for the two types of minihole in the Southern Hemisphere). Thus, a high positive correlation between the total ozone and geopotential height in the lower stratosphere suggests an air mass originating from the polar vortex.

Figure 3 shows the Hovmöller diagrams for the wavenumber 1 and 2 components of the geopotential height at 50–60°S and 50 hPa, during the period from 1 October to 31 December in 2009, along with those in 1980, 1997, and 2011, in which the minimum phases of wavenumbers 1 and 2 were also observed near Rio Gallegos, and those of the composite from 1979 to 2015, for comparison. Figure 4 shows the Hovmöller diagrams for the wavenumber 1 and 2 components of the total ozone from TOMS/OMI at 50–60°S. This latitude range includes Rio Gallegos (51.5°S, 69.3°W). The wavenumber 1 and 2 components of the total ozone in 2009, 1980, 1997, and 2011 in Figures 4a, 4c, 4d, and 4e indicate temporal and longitudinal high positive correlations with those of the geopotential height at 50 hPa shown in Figures 3a, 3c, 3d, and 3e, respectively, in October and November. The positive correlations in October and November suggest variations caused by low temperatures and the ozone-poor air mass of the ozone hole or an air mass originating from it.

As shown in Figure 3b, the minimum phase of wavenumber 1 of the composite geopotential height for 1979–2015 is located around 0°E during October–December. In 2009, wavenumber 1 is considered to have remained quasi-stationary with a minimum phase around 0–30°E and a maximum phase around 180–150°W in October and in the middle and end of December, as indicated in Figure 3a. However, the minimum phase longitude in November 2009 is considerably different from those in the 37-year climatology series. The minimum phase is located near the longitude of Rio Gallegos, indicated by the dashed vertical line. The minimum phase of the geopotential height corresponds to that of the total ozone, as shown in Figure 4a.

As shown in Figures 3c, 3d, and 3e, we found three other years (1980, 1997, and 2011) in which the minimum phase of wavenumber 1 of the geopotential height was located near the longitude of Rio Gallegos in November for all 37 years 1979–2015, although their minimum phase was located slightly west of the longitude of Rio Gallegos. The minimum phase of wave number 1 of the total ozone was also located there (Figures 4c, 4d, and 4e). These 3 years are discussed later in section 7, together with other years in the period 1979–2015.

It is well known that the phase of zonal wavenumber 2 in the Southern Hemisphere stratosphere predominantly travels eastward with a period of 10–20 days (e.g., Harwood, 1975). Because wavenumber 2 is not a stationary wave but a traveling wave, the composite for the 37 years has a very small amplitude due to the cancelation among the components for all years, but some evidence of the eastward movement can be seen in October and in the first half of November (right panel of Figure 3b). The wavenumber 2 component of the composite of the geopotential height does not show a high correlation with the wavenumber 2 component

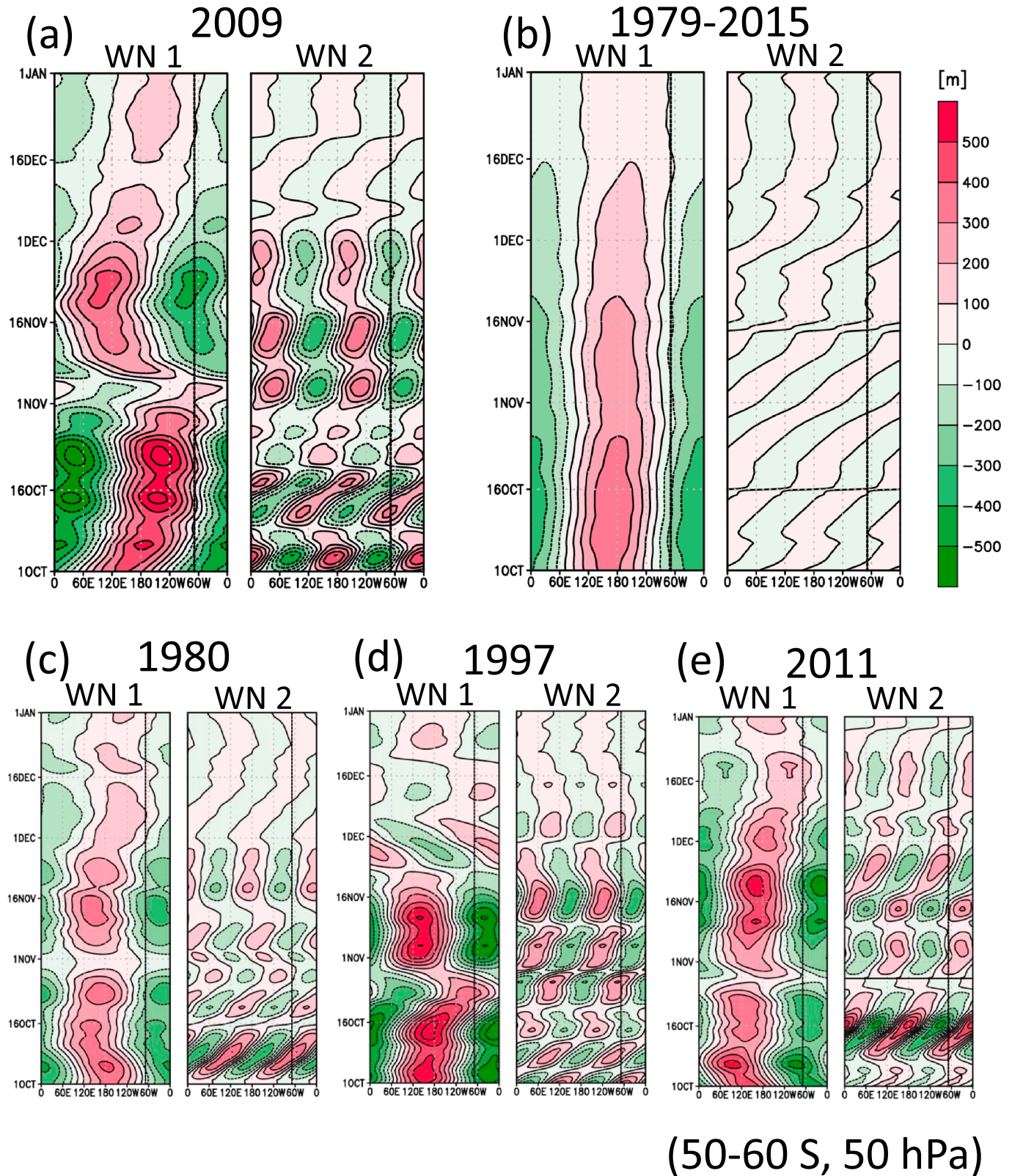


Figure 3. Hovmöller diagram of the wavenumber 1 (left panels) and 2 (right panels) components of the geopotential height at 50–60°S and 50 hPa for ERA-Interim, from 1 October to 31 December in 2009 (a), the composite for 1979–2015 (b), 1980 (c), 1997 (d), and 2011 (e). The value of the wave component is indicated using red for positive values and green for negative values. The longitude of Rio Gallegos is designated by the vertical black solid line at 69.3°W.

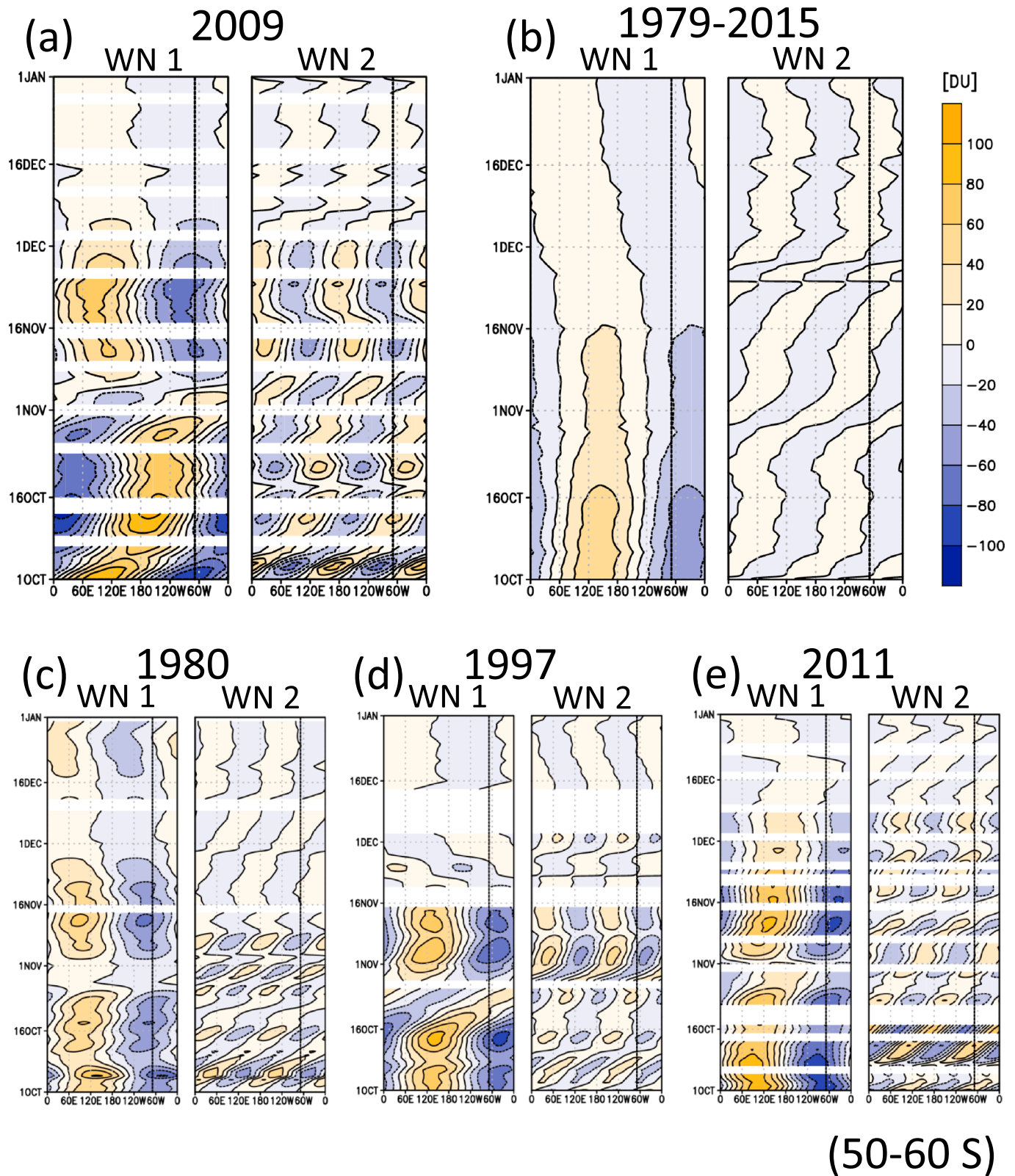


Figure 4. Same as Figure 3, but for the wavenumber 1 (left panels) and 2 (right panels) components of the total ozone from the Total Ozone Mapping Spectrometer/ Ozone Monitoring Instrument at 50–60°S. The value of the wave component is indicated using orange for positive values and blue for negative values.

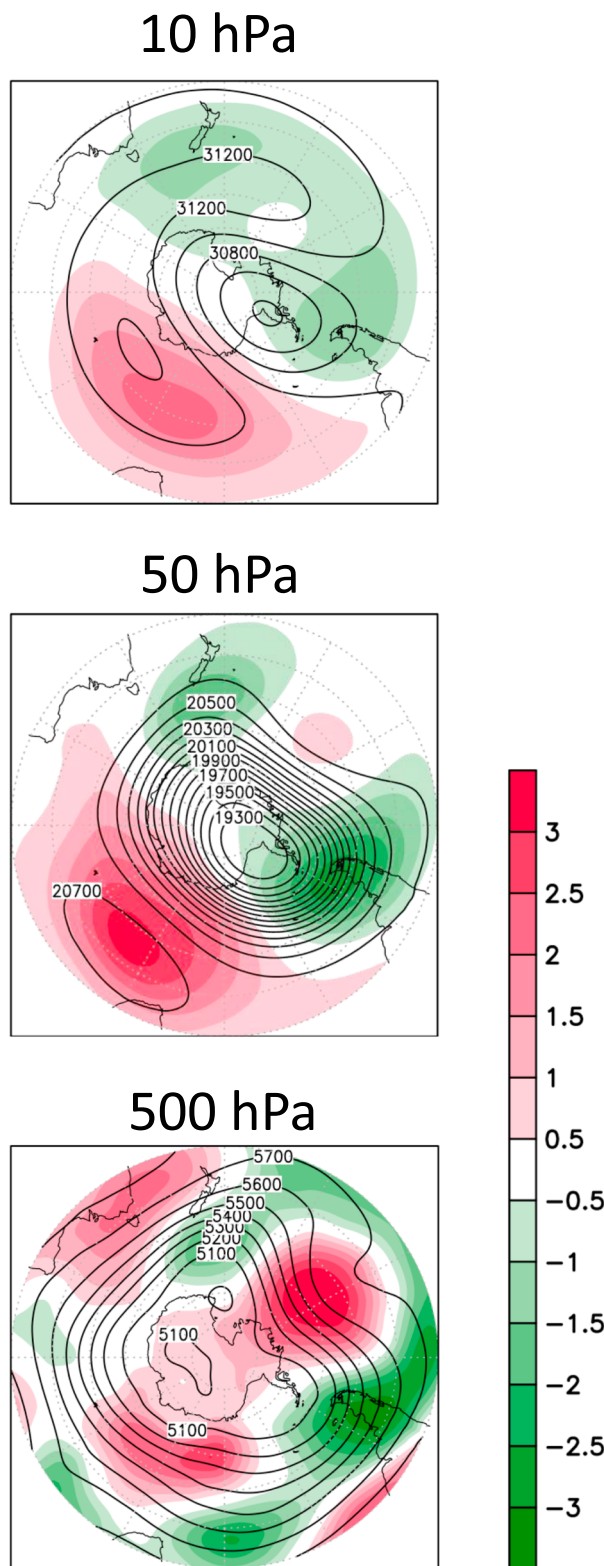


Figure 5. The geopotential height distribution in November 2009 (contour) and its anomaly from the 37-year-mean (color) in the Southern Hemisphere at 10 (top), 50 (middle), and 500 hPa (bottom). The anomaly is normalized by the standard deviation from the climatology at each grid point.

of the composite of the total ozone. In mid-October 2009, the phase of zonal wavenumber 2 traveled eastward, as in the climatology (right panel of Figure 3a). However, in late October, the phase speed decreased. Consequently, the negative anomaly of zonal wavenumber 2 was located over the longitude of South America throughout November. This behavior for wavenumber 2 of the geopotential height is different from the climatology.

Considering that wave number 1 is mainly associated with a shift of the polar vortex from the South Pole and wave number 2 is associated with the elongation of the polar vortex around the South Pole, the development of wavenumber 2 with wavenumber 1 was important for the elongated vortex edge to reach the southern part of the South American continent in November 2009.

6. Analyses of Processes Associated With a Connection Between the Stratosphere and Troposphere

Figure 5 shows the normalized geopotential height anomaly at 10, 50, and 500 hPa in November 2009 from the climatology for 1979–2015. A large positive anomaly of more than three standard deviations (the maximum value is 3.67) is evident around 120°W at 500 hPa. At the upper levels of 10 and 50 hPa, large negative anomalies over the South American continent are evident. The minimum value at 50 hPa is -2.80 standard deviations. It is suggested that the large positive anomalies in the troposphere and the large negative anomalies in the stratosphere have some relation.

Figure 6 shows height-longitude cross sections of Plumb's wave activity flux and the geopotential height anomaly from the zonal mean at 50–60°S on 9, 11, and 13 November 2009. These values were calculated using the ERA-Interim reanalysis data and the method of Plumb (1985). The figure indicates that a large wave activity flux originating around 120°W in the troposphere is propagating into the stratosphere on 9 and 11 November (top and middle panels), where a large negative geopotential height anomaly developed around 60°W (near Rio Gallegos) on 11 and 13 November (middle and bottom panels). The wave propagation is also evident from the westerly tilted contours of the geopotential height at 60–120°W on these days (the vertical structure tilts westward with increasing height).

Figure 7 indicates longitudes where blocking patterns occurred at 500 hPa for a latitude range of 30–65°S as a function of time in November 2009 in accordance with the method of Mendes et al. (2008, 2012); see also Tibaldi et al. (1994) for details on the method. In this diagnosis, the latitudinal gradients of the geopotential height were examined. The gradients of the daily geopotential height between 55°S and 40°S and those between 65°S and 50°S were investigated. If the former is positive and the latter is less than -10 m/degree, then the geopotential height field was diagnosed as showing a blocking pattern at a specific instant in time. This process was repeated at intervals of 2.5° in latitude until the north edge was at 30°S and was performed at every longitude for the data in November. The large positive anomaly in the November-mean geopotential height field at 500 hPa shown in the bottom panel of Figure 5 was a result of the frequent occurrence of blocking patterns in the daily geopotential height field in November (Figure 7). Figure 7 indicates that a blocking pattern was present at 120–150°W on 1–6

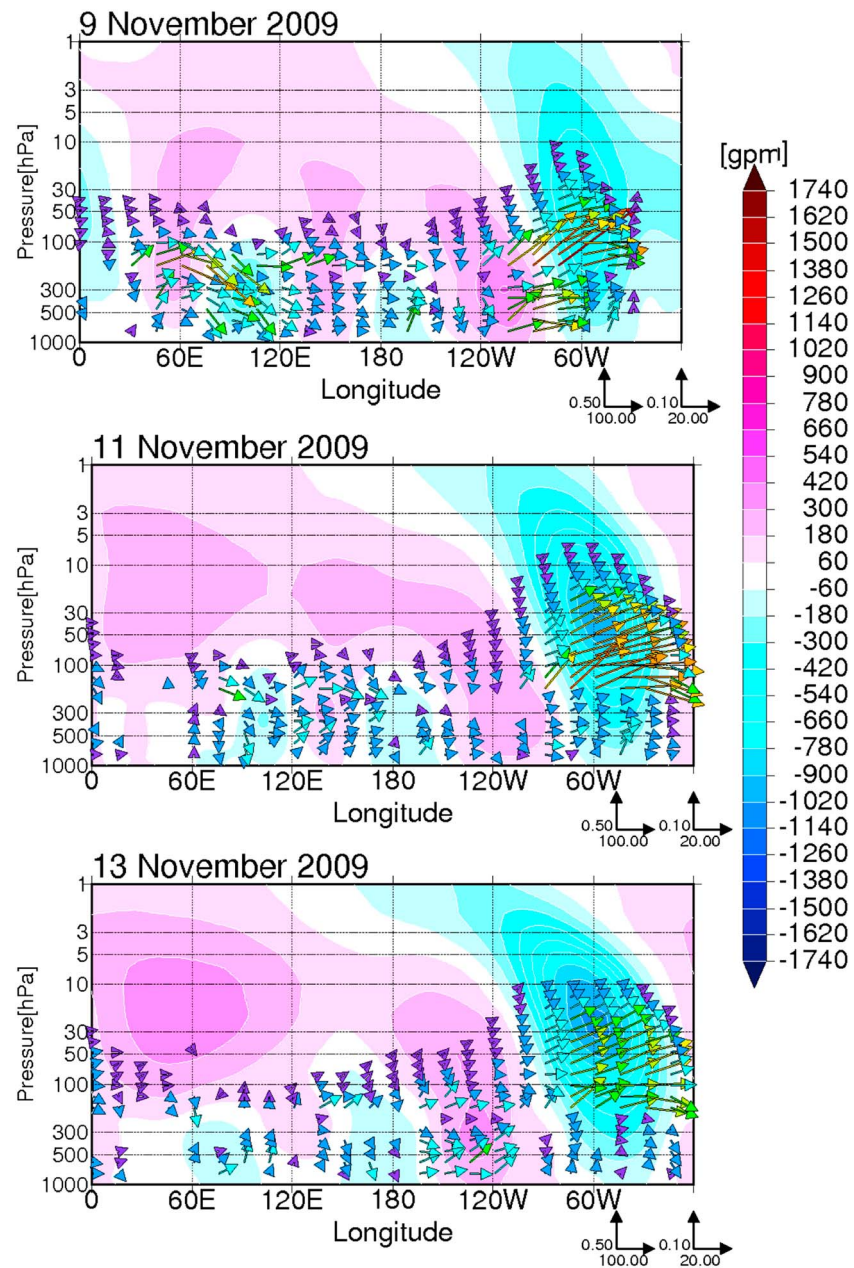


Figure 6. Wave activity flux (arrows) and geopotential height anomaly from the zonal mean (color) at 50–60°S on 9, 11, and 13 November 2009. The scales for the wave activity flux are represented at the bottom; the left scale is for pressure levels below 200 hPa (for the troposphere), and the right scale is for those above 200 hPa (for the upper troposphere and stratosphere). The length of the arrows is proportional to the flux, and the arrows are colored depending on the magnitude of the flux for conspicuousness.

November and around 90°W on 8–10 November. Accordingly, the wave activity flux from the troposphere to the stratosphere was enhanced on 8–11 November and a negative geopotential height anomaly developed in the stratosphere around 60°W on 8–13 November (Figures 6 and 3a). The wave propagation was also evident from the westerly tilted contours of the geopotential height at 60–120°W on these days, as shown in Figure 6. Thus, the large negative anomaly is associated with polar vortex migration (Figures 8 and 2). Also, a blocking pattern was present on 13–15 November around 120–165°W, on 19–23 November around 120–150°W, and 25 November–1 December around 120°W. Enhanced wave activity flux from the troposphere to the stratosphere was evident around 120°W on 20–30 November.

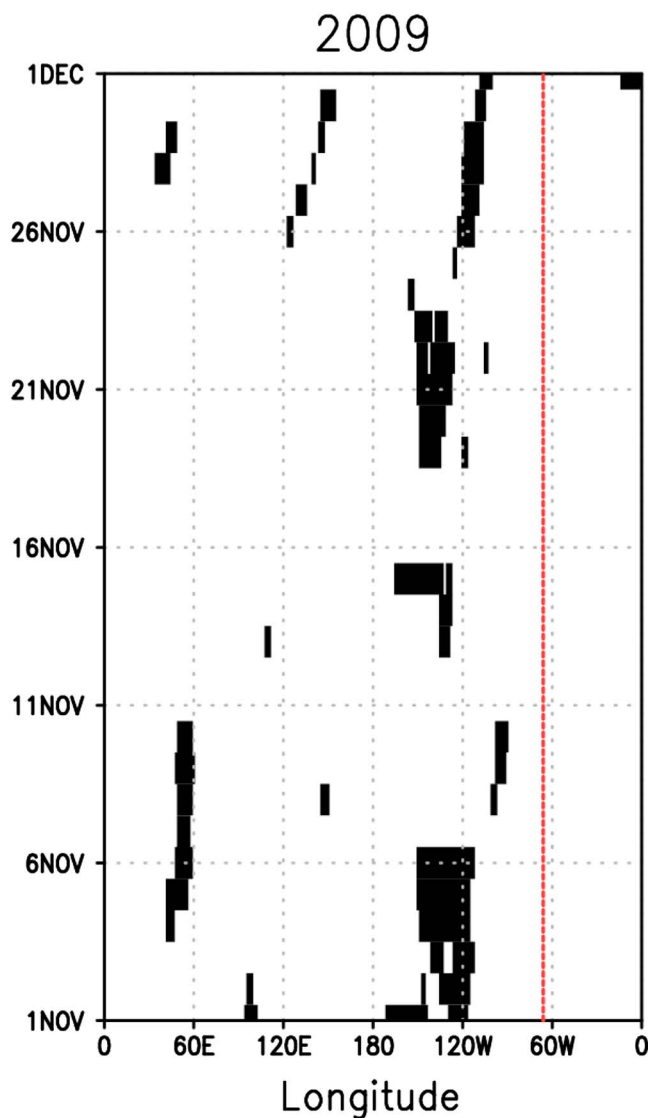


Figure 7. Longitudes where blocking patterns occurred at 500 hPa in the Southern Hemisphere in November 2009 indicated by solid black as a function of the date from 1 November to 30 November. The longitude of the large negative geopotential height anomaly at 50–60°S and 50 hPa in November 2009 (see Figure 10) is designated by the vertical red dashed line.

Because diagnosis of the blocking patterns was performed following the method of Mendes et al. (2008, 2012), which used the National Centers for Environmental Prediction/National Center for Atmospheric Research reanalysis grid ($2.5^\circ \times 2.5^\circ$ in latitude and longitude), we linearly interpolated the ERA-Interim data from a resolution of $1.5^\circ \times 1.5^\circ$ to a resolution of $2.5^\circ \times 2.5^\circ$. To confirm that the interpolation does not significantly influence the blocking pattern diagnosis, we repeated the diagnosis of blocking events using the ERA-Interim data without any spatial interpolation but with a slightly modified latitude range and conditions for the diagnosis of a blocking pattern (see section 1 and Figure S1 in the supporting information). The longitude-latitude distribution of the geopotential height at 500 hPa on 9 November 2009 (one of the days diagnosed as blocked and shown in the top panel of Figure 6) is also shown in Figure S2, where a blocking pattern is evident around 60° – 120° W in the latitude range of 30° S– 66° S when the wave activity flux from the troposphere to the stratosphere was enhanced. Although there are some differences between Figures 7 and S1 (e.g., the geopotential height field on 10 November 2009 was not diagnosed as blocked in Figure S1), the differences are insignificant, and the result that blocking patterns were often found to the west of the South American continent in November 2009 is unchanged.

7. Dynamical Field and Total Ozone at 50–60°S for the 37-Year Period of 1979–2015

7.1. Location of the Antarctic Polar Vortex Before the Breakup During 1979–2015

Because the 2009 low total ozone event over Rio Gallegos was associated with the Antarctic polar vortex breakup process, we examined the geographical distribution of the polar vortex breakup by analyzing the longitude-latitude distribution of the cumulative number of days the polar vortex existed during the week before the breakup date for the 37-year period of 1979–2015 (Figure 9). The ERA-Interim data were used for the analysis. The day of the polar vortex breakup was defined as the day when the -32 PVU contour at 450 K encloses an area of less than 5×10^6 km², as was done at the National Centers for Environmental Prediction to calculate the Southern Hemisphere polar vortex vanishing date (www.cpc.ncep.noaa.gov/products/stratosphere/winter_bulletins/sh_10/Fig_7.gif).

Because the Antarctic polar vortex breaks up not only in November but also occasionally in October and December, the analysis provides the distribution of the vortex air with low ozone just before the breakup,

independent of the month. The figure indicates that the vortex breakup occurred more commonly in the South America-Atlantic Ocean-Indian Ocean longitudinal section at 50–60°S, which indicates that the low-ozone air mass of the polar vortex tended to stay in or flowed out to this longitudinal section more frequently. This result is consistent with the croissant shape of the climatological maximum total ozone on the Indian Ocean side and the minimum on the Pacific Ocean side (left panel of Figure 4b), which reflects the climatological wavenumber 1 planetary wave structure with the maximum phase around 180° E and the minimum phase around 0° E (left panel of Figure 3b).

7.2. Analysis of the 50-hPa Geopotential Height and the Total Ozone at 50–60°S for 1979–2015

During the period between 1979 and 2015, there were a few cases of extremely low geopotential height occurring in the lower stratosphere around South America. Figure 10 shows the geopotential height anomaly from the 1979–2015 mean at 50–60°S and 50 hPa in November, normalized by the standard deviation at each longitude. The analysis indicates that negative anomalies of less than -2.5 standard deviations occurred in

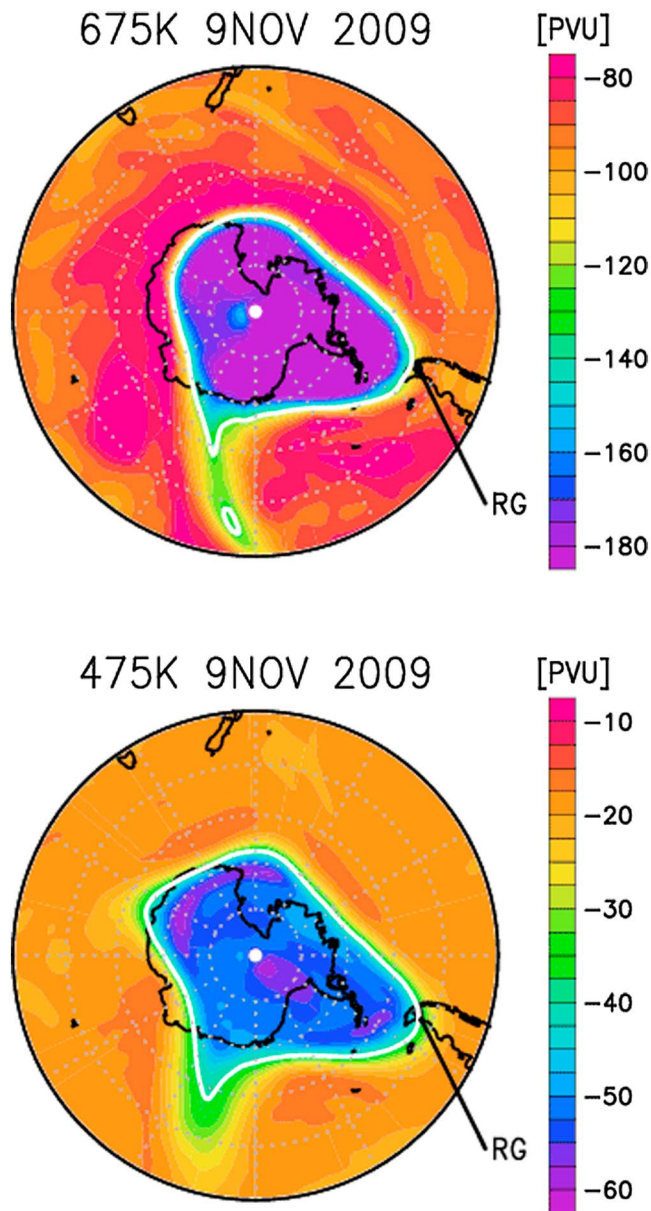


Figure 8. Same as Figures 2c and 2e, but for 9 November 2009. The potential vorticity distribution at 675 K (upper panel) and that at 475 K (lower panel).

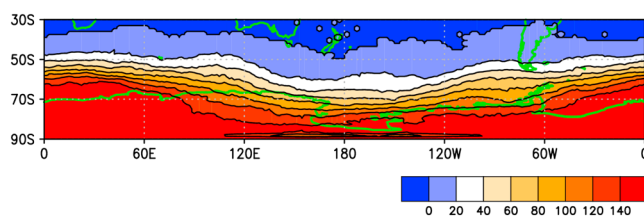


Figure 9. Distribution of the cumulative number of days the polar vortex existed in the week before polar vortex breakup for the 37 years of 1979–2015. The ERA-Interim data are used for the analysis. The number of days is indicated by color. The coastline is denoted by light-green lines.

1987, 1997, 2001, and 2009. The mean total ozone distribution in the Southern Hemisphere in November for these 4 years and those for 1980 are shown in the figure. The geopotential height anomaly in 1980 is not very large but has similar distributions of ozone and geopotential height to those in 2009, as described later in this section. The years 1994 and 2001 have anomalies of more than -2.0 standard deviations. Around 60°W and $50^\circ\text{--}60^\circ\text{S}$ near Rio Gallegos, negative anomalies of less than -2.5 standard deviations occurred in 2009 and 1997. These negative anomalies are associated with low total ozone in this region, as shown by the total ozone maps in the figure. In 1997, however, a large geopotential height anomaly was not exactly located at the Rio Gallegos longitude but at longitudes slightly eastward over the Atlantic Ocean. Furthermore, the period of low total ozone associated with the large negative anomaly in the 50-hPa geopotential height only lasted for 2 weeks in November. Negative anomalies in wavenumber 1 were evident around 30°W , though only in the first half of the month (left panel of Figure 3d).

Large negative anomalies of less than -2.5 standard deviations were evident in 1987 and 2001 as well as in 2009 and 1997 (Figure 10). However, these geopotential height anomalies were located around 130°W and 70°E , respectively, so the low total ozone corresponding to these anomalies did not affect the South American continent.

Figure 11 shows the anomaly of the total ozone from TOMS/OMI for the 1979–2015 mean at $50^\circ\text{--}60^\circ\text{S}$ in November. Large negative anomalies of less than -2.0 standard deviations around Rio Gallegos are evident in 1997 (-2.6 standard deviations at 35.0°W), 2009 (-2.4 standard deviations at 77.5°W), and 2011 (-2.3 standard deviations at 92.5°W), although the geopotential height anomaly in 2011 is not very large (Figure 10). These 3 years are shown in Figure 4 for the wavenumber 1 and 2 components of the total ozone. Apart from Rio Gallegos, negative anomalies of less than -2.0 standard deviations are evident in 2001 and 2013, which correspond to the negative anomalies in the geopotential height around 70°E and 120°E in Figure 10, respectively.

In 1980, a negative anomaly for wavenumber 1 of the geopotential height was located slightly to the east of Rio Gallegos during the middle of November (left panel of Figure 3c). This created a weak negative total ozone anomaly around Rio Gallegos (Figure 4c). The longitude-time cross sections of the wavenumber 1 and 2 components of the geopotential height are similar to those observed in November 2009, although the amplitude is smaller (Figure 3c). Accordingly, the total ozone anomaly is smaller than that observed in November 2009 (Figures 12a and 12c). The reason for this is that the ozone hole over Antarctica had not yet substantially developed in 1980. Thus, a long-lasting period of low total ozone did not occur over the South American continent in the late spring of 1980. However, that event may be noteworthy because it was a dynamical field in which the Antarctic polar vortex was elongated and migrated in the direction of South America. If the concentration of ODS in the atmosphere had been high under the dynamical field of 1980, a long-lasting period of low total ozone would have occurred over South America. We have confirmed this by means of a numerical experiment using the CCSRNIES MIROC3.2 CCM (see Akiyoshi et al., 2016, for details of the model). The horizontal wind speeds and temperature were nudged toward those of the ERA-Interim reanalysis data for 1980, while concentrations of ODS from the year 2000 were used. Figure 12 shows the observed and simulated

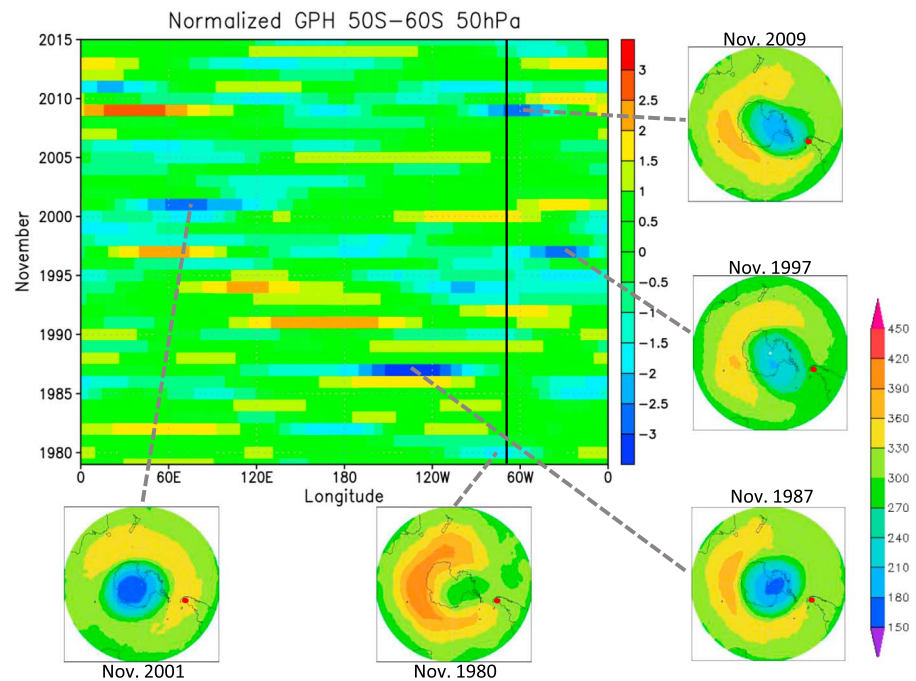


Figure 10. Geopotential height (GPH) anomaly from the 1979–2015 mean at 50–60°S and 50 hPa in November, normalized by the standard deviation at each longitude. The magnitude of the anomaly is indicated by its color. The longitude of Rio Gallegos is designated by a solid vertical black line at 69.3°W. The mean total ozone distribution in the Southern Hemisphere in November for the years when the normalized geopotential height anomaly is less than -2.5 , and those of 1980 are also shown using polar maps with the color scale in Dobson units. The location of Rio Gallegos is designated by red dots in the polar maps.

total ozone at 50–60°S from October to December 2009 and 1980. From a comparison of Figures 12a and 12b for 2009, and Figures 12c and 12d for 1980, the model can be seen to simulate the total ozone variation and distribution very well. The result of the simulation with the wind and temperature for 1980 and ODSs for 2000 is shown in Figure 12e, where a low total ozone event over Rio Gallegos is evident for about 3 weeks in November as in the 2009 event in Figure 12b.

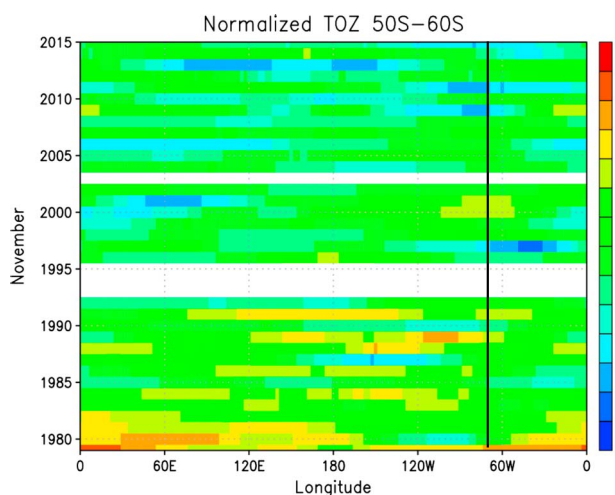


Figure 11. Total ozone (TOZ) anomaly from the Total Ozone Mapping Spectrometer/Ozone Monitoring Instrument for the 1979–2015 mean at 50–60°S in November, normalized by the standard deviation at each longitude. The magnitude of the anomaly is indicated by its color. White indicates missing data. The longitude of Rio Gallegos is designated by a solid vertical black line at 69.3°W.

Figure 13 shows a histogram of the total ozone anomaly for 50–60°S and 65–75°W in November from the 1979–2015 mean of TOMS/OMI. Rio Gallegos is located within this region. This histogram is equivalent to the distribution of the total ozone anomaly along the longitudes 65–75°W including the vertical black line at 69.3°W in Figure 11. In this region around Rio Gallegos, there were 2 years when the standard deviation was less than -2.0 (2009 and 2011) out of the 37 years between 1979 and 2015, as shown in Figure 13. In 2009, as shown in Figure 1, the total ozone had low values under 300 DU over 25 days from 9 November to 3 December after high values of around 370 DU on the first several days in November. In 2011, the total ozone was under 300 DU for 15 days from 9 November to 23 November after having values around 300 DU in early November. In particular, the total ozone on 17 and 20 November showed very low values under 220 DU (182 and 210 DU, respectively) owing to the transit of the vortex air. Thus, the period when the total ozone was less than 300 DU was shorter than that in 2009. Although these 2 years have the same classification of negative anomaly as the November-mean total ozone in Figure 13, the negative anomaly in November 2009 is one of the largest anomalies in magnitude and duration for the 37 years in association with the large negative geopotential height anomaly.

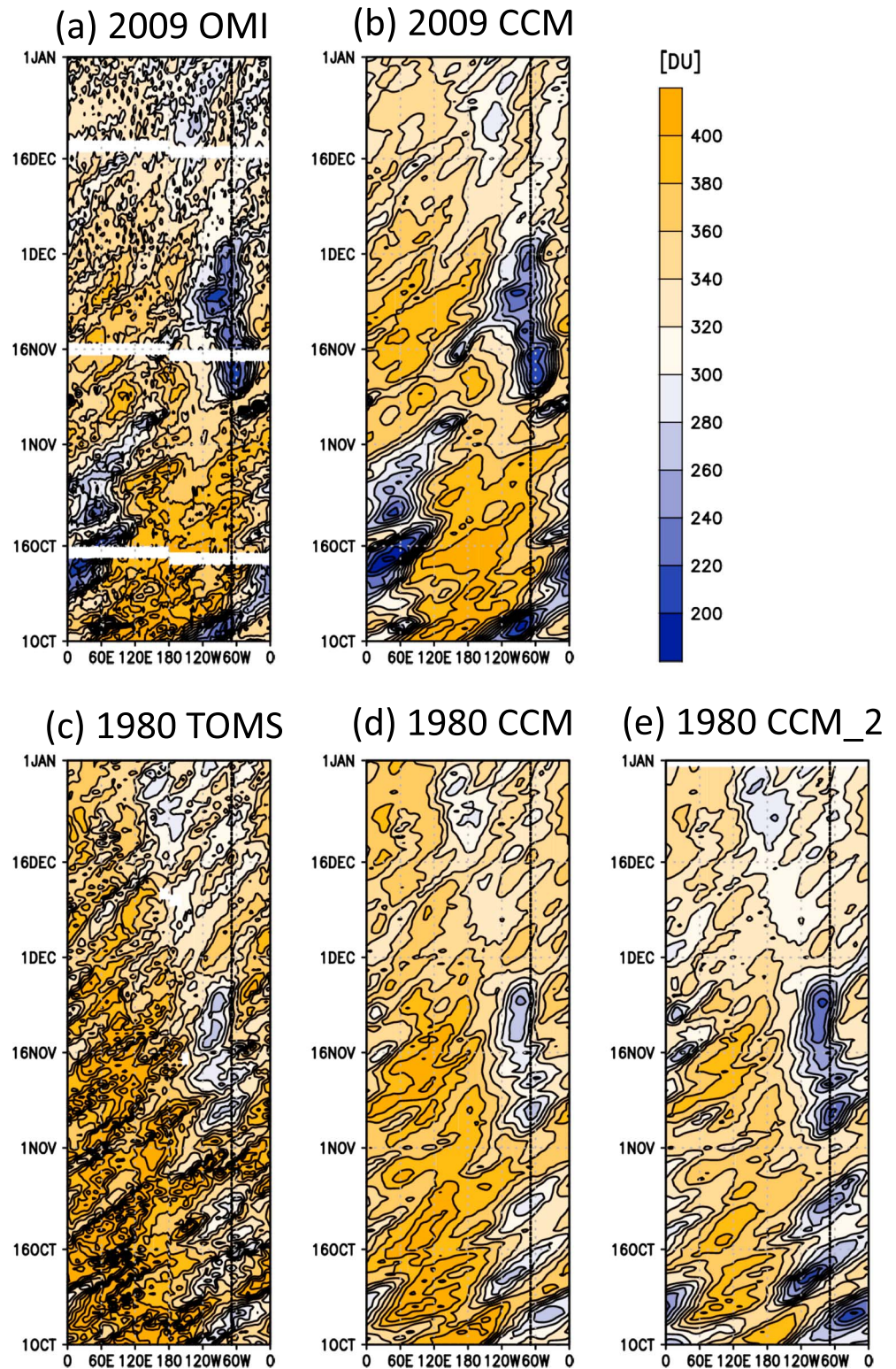


Figure 12. Longitude-time cross section of the total ozone at 50–60°S in October–December 2009 (upper panels) and 1980 (lower panels). The total ozone amount is represented by the color scale in Dobson units (DU). The longitude of Rio Gallegos is designated by the vertical black solid line at 69.3°W. (a) Observations in 2009 by the Ozone Monitoring Instrument (OMI). (b) Simulations for 2009 by the nudged chemistry-climate model (CCM). (c) Observations in 1980 by the Total Ozone Mapping Spectrometer (TOMS). (d) Simulations for 1980 by the nudged CCM. (e) Simulations for 1980 by the nudged CCM with ozone depleting substance concentrations for 2000.

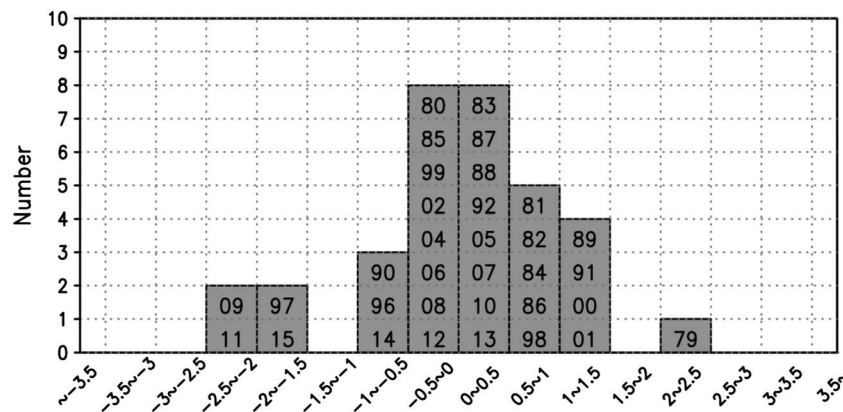


Figure 13. Histogram of the total ozone anomaly at 50–60°S and 65–75°W in November from the 1979–2015 mean of the Total Ozone Mapping Spectrometer/Ozone Monitoring Instrument. The anomalies are normalized by the standard deviation. The numbers in the panel denote the years (“79” denotes the year 1979, and “09” denotes the year 2009). The mean value of the total ozone in this region is 322 DU, and the standard deviation is 22.0 DU.

7.3. Analyses of Blocking Patterns at 500 hPa and Wave Activity Flux in the Years of Large Negative Geopotential Height Anomalies in the Stratosphere

Concerning the effect of the troposphere, the relationship between Antarctic polar vortex migration toward the Southern Hemisphere lower latitudes at the time of the polar vortex breakup and the blocking event in the Southern Hemisphere troposphere was examined for several years showing large negative geopotential height anomalies in the stratosphere. In the Northern Hemisphere, the relationship between sudden stratospheric warming and blocking events in the troposphere, and the role of wavenumbers 1 and 2 has been widely investigated and discussed (e.g., Castanheira & Barriopedro, 2010; Labitzke, 1965; Nishii et al., 2011; Quiroz, 1986; Taguchi, 2008). Some studies indicated that sudden stratospheric warming events in the Northern Hemisphere were preceded by blocking (e.g., Bancelá et al., 2012; Harada et al., 2010; Martius et al., 2009). This may suggest that monitoring blockings may lead to improved forecasts of the vortex behavior associated with sudden stratospheric warmings and, thus, polar vortex breakup (e.g., Mukougawa et al., 2005, 2007), conditional on the ability of the models to accurately simulate blocking. In this study, we focus on the Southern Hemisphere in November when the Antarctic polar vortex is breaking up or in the conditions immediately preceding the breakup.

We examined whether blocking phenomena occurred in the November geopotential height distributions at 500 hPa in the Southern Hemisphere troposphere in the years of the large negative geopotential height anomalies at 50 hPa (i.e., 1987, 1997, 2001, and 2009). This was done using the diagnosis method of Mendes et al. (2008, 2012) for a latitude range of 30–65°S as was done for 2009 in section 6. Figures 14a–14c show that blocking patterns were diagnosed in the troposphere to the west of the large negative geopotential height anomaly at 50 hPa in 1987, 1997, and 2001. The durations of the blocking patterns in November of these years were somewhat shorter or much shorter than that in 2009 in Figure 7. In 1987, blocking patterns were diagnosed to the west of the large negative geopotential height at 50 hPa around 180°E on 17–27 November (Figure 14a), and enhanced wave activity flux from the troposphere to the stratosphere and the development of a negative geopotential height anomaly around 130°W in the stratosphere were evident on 18–22 November (Figure 15a), and a polar vortex elongation to this longitude section occurred on these days (Figure 16a).

In 1997 and 2001, blocking patterns were evident to the west of the large negative geopotential height at 50 hPa for a few days on 2–5 and 6 November 1997 and 12–16 November 2001 (Figures 14b and 14c). Accordingly, an enhancement of the wave activity flux from the troposphere to the stratosphere was evident on these days, and negative anomalies in the stratosphere around 40°W in 1997 and 50°E in 2001 developed (Figures 15b and 15c). In 1997, the polar vortex migrated in the direction of 40°W at the beginning of November (Figure 16b), corresponding to the days with blocking. In 2001, migration occurred in the direction of 50°E around the days with blocking (Figure 16c), but it was not the only migration that occurred in November in this year.

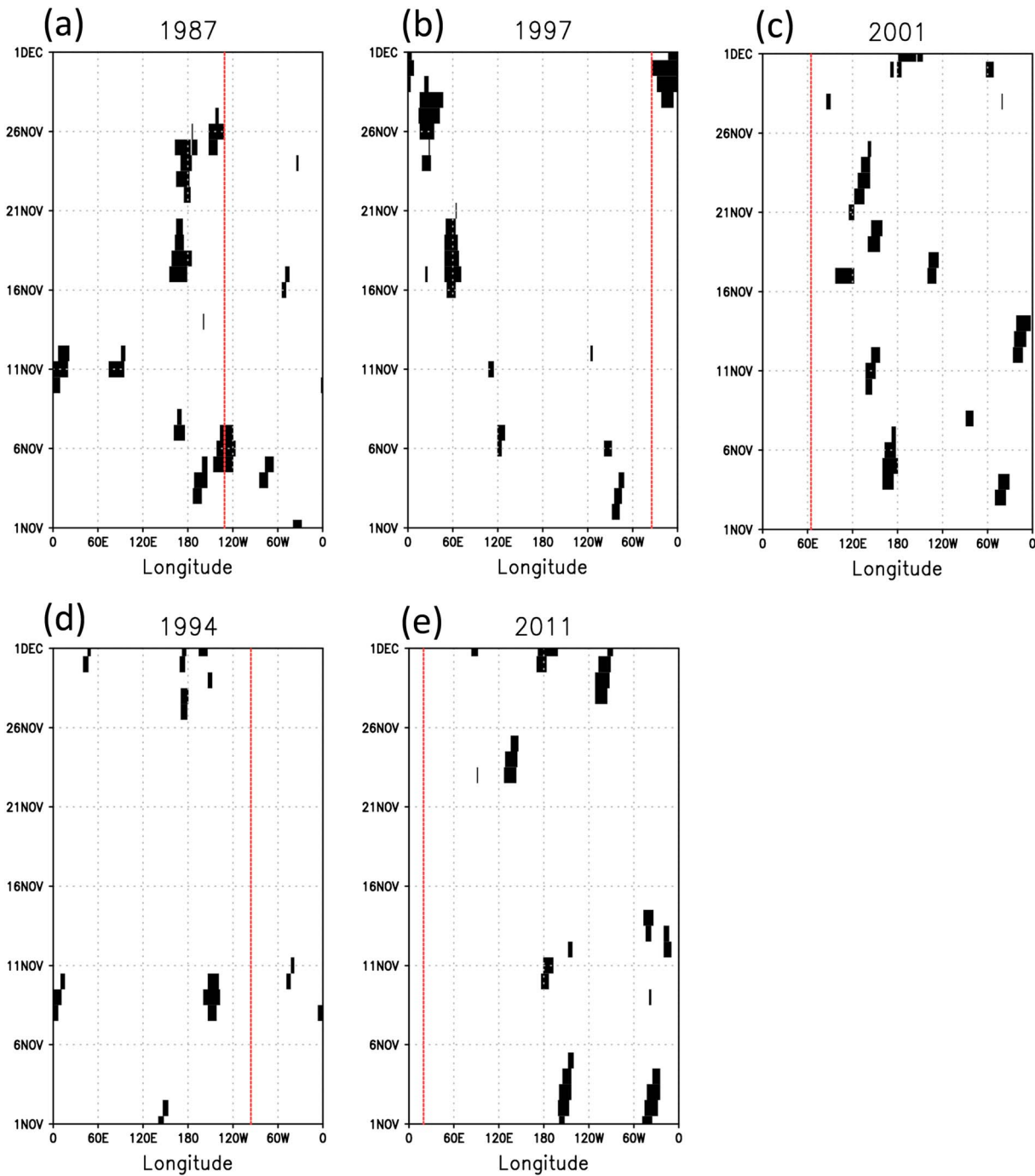


Figure 14. Same as Figure 7, but for November 1987 (a), 1997 (b), 2001 (c), 1994 (d), and 2011 (e). The longitude of the large negative geopotential height anomaly at 50–60°S and 50 hPa in each year (see Figure 10) is designated by the vertical red dashed line.

In addition, in 1994 and 2011, the geopotential height anomalies were not as large as those for the above 4 years, but they show large negative anomalies of less than -2.0 standard deviations (Figure 10), and blocking patterns in the troposphere to the west of the negative geopotential height anomaly at 50 hPa are diagnosed on 8–10 November 1994 and 12–14 November 2011, as shown in Figures 14d and 14e. The wave activity flux from the troposphere and stratosphere was enhanced, and accordingly, negative anomalies in the stratosphere around 100°W in 1994 and 30°E in 2011 developed (Figures 15d and 15e). Then, the polar vortex tended to migrate toward lower latitudes at these longitude sections on these days (Figures 16d and 16e).

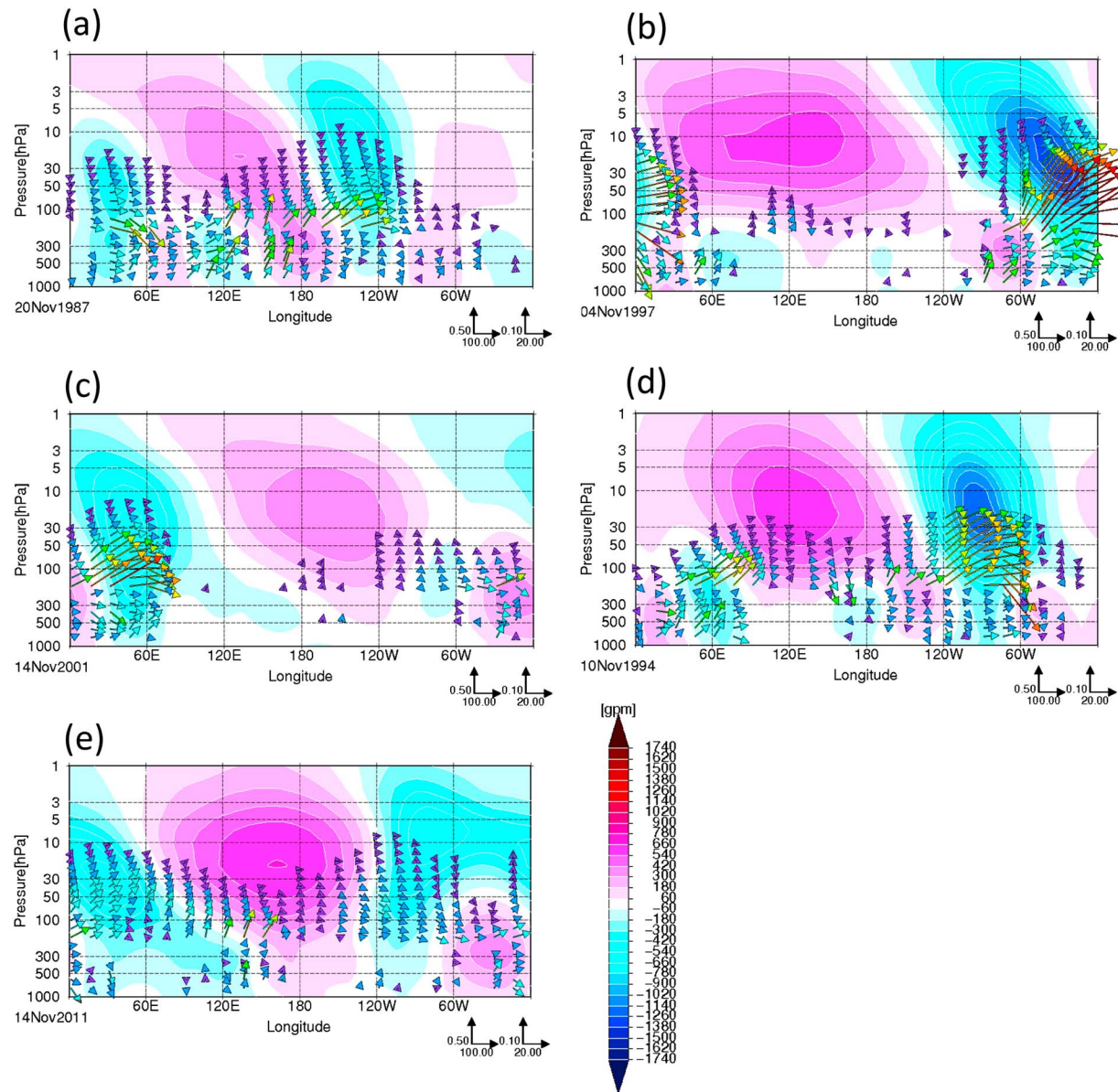


Figure 15. Same as Figure 6, but for 20 November 1987 (a), 4 November 1997 (b), 14 November 2001 (c), 10 November 1994 (d), and 14 November 2011 (e).

As in section 6, we also diagnosed the blocking patterns in November of these years using the ERA-Interim data with a resolution of $1.5^\circ \times 1.5^\circ$ in latitude and longitude and with a modified latitude range and conditions for the diagnosis. The results are shown in Figure S3 in the supporting information. The longitude-latitude distributions of the geopotential height at 500 hPa for one of the days diagnosed as blocked in each year (the days of the years in Figures 15 and 16) are shown in Figure S4. From the longitude-latitude distributions of the geopotential height, a blocking pattern is evident around the days when the wave activity flux from the troposphere to the stratosphere was enhanced. As in 2009, although there are some differences between Figures 14 and S3, the differences are insignificant, and our conclusion is unchanged that blocking patterns were diagnosed to the west of large negative anomalies in the stratosphere in association with the enhanced wave activity flux from the troposphere to the stratosphere.

These results suggest that for the years showing large negative geopotential height anomalies at 50 hPa in November, blocking patterns occurred for up to several days in the Southern Hemisphere troposphere to the west of the large negative geopotential height anomalies in the stratosphere in association with the

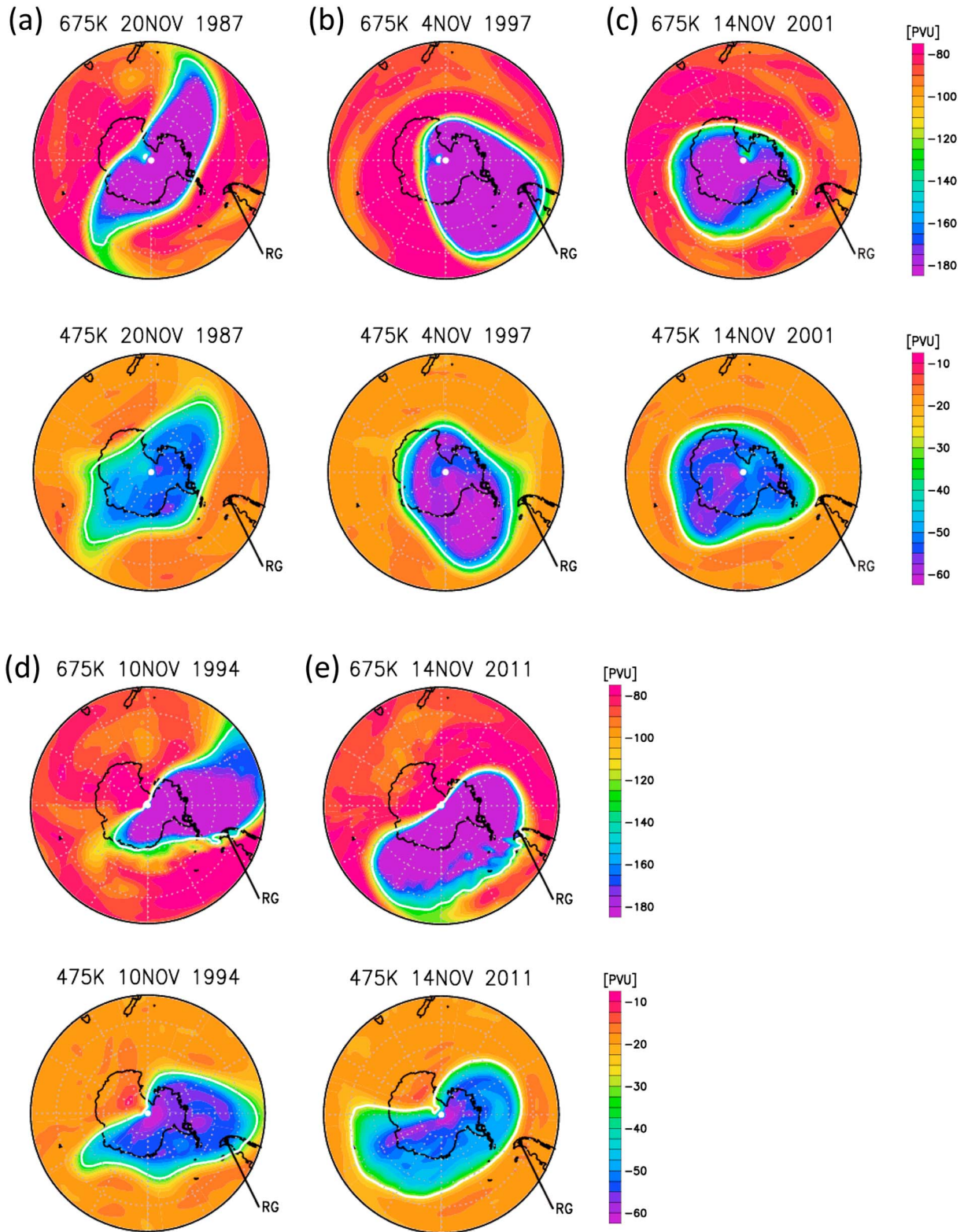


Figure 16. Same as Figures 2c and 2e, but for 20 November 1987 (a), 4 November 1997 (b), 14 November 2001 (c), 10 November 1994 (d), and 14 November 2011 (e). The potential vorticity distributions at 675 K (upper panels) and those at 475 K (lower panels).

polar vortex migration from the pole to the lower latitudes. The frequency and duration of blocking patterns in November 2009 were much higher and longer than those of 1987, 1997, 2001, 1994, and 2011. However, not all large negative geopotential height anomalies in the stratosphere and polar vortex migrations were associated with blocking.

8. Conclusions

We investigated the total ozone distribution and the dynamical field at 50–60°S around Rio Gallegos (51.5°S, 69.3°W) in November 2009, when a long-lasting low total ozone event was observed there. A low-ozone event also occurred in October. In October, however, the main driver of the low-ozone event was the movement of the edge of the elongated polar vortex, which resulted in a reduction of the total ozone lasting several days.

Our analyses of the ERA-Interim reanalysis data indicate that a several-week reduction of the total ozone was caused by the polar vortex migrating toward the South American continent at the time of the vortex breakup. The polar vortex migration and the development of the negative geopotential height anomaly in the stratosphere were associated with an enhanced wave flux from the troposphere to the west of South America to the stratosphere over the southern part of the continent. Furthermore, the enhanced wave flux propagation and blocking in the troposphere to the west of the South American continent occurred almost simultaneously in the timescale of a few days to several days, where a large positive anomaly of more than three standard deviations of the 500-hPa geopotential height from the climatology for 1979–2015 was evident around 120°W in November. The blocking and wave propagation resulted in a large negative anomaly of less than -2.5 standard deviations of the geopotential height at 50 hPa and of less than -2.0 standard deviations of the total ozone over the South American continent at 50–60°S in November 2009.

We also investigated the total ozone and the dynamical field for the period from 1979 to 2015. Our analyses of the geopotential height at 50 hPa in November for the past 37 years indicate that the large negative anomaly of less than -2.5 standard deviations in the lower stratosphere around South America occurred only in 1997 and 2009. In 1997, the polar vortex migrated toward the South American continent before its breakup and caused a period of low-ozone amount, but for a shorter period than in 2009. The large negative anomaly in 1997 was also associated with blocking in the troposphere, but the period diagnosed as blocked was much shorter than that in 2009. An enhancement of the wave activity flux from the troposphere to the stratosphere was evident in association with the blocking. In addition to 1997 and 2009, a nudged CCM simulation demonstrated that if the concentration of ODSs in the atmosphere had been high under the dynamical field of 1980, a long-lasting period of low total ozone would have occurred over South America as in 2009.

In addition to the years with large negative geopotential height anomalies at 50–60°S around South America, in 1987, 2001, 1994, and 2011, there were very large negative geopotential height anomalies of less than -2.0 standard deviations in different locations (longitudes). For these years, total ozone also shows large negative anomalies near the longitudes except for the year 1994, when the TOMS data were missing. The negative total ozone anomaly in November 2011 was categorized as being in the same range as 2009 in our analysis, but the period when the total ozone was less than 300 DU was shorter than that in 2009. The geopotential height anomaly in November 2011 was less than -2.0 standard deviations and smaller than those in 2009 and 1997.

In association with the enhanced wave activity flux from the troposphere to the stratosphere, blocking patterns were evident for up to several days in the years showing large negative geopotential height anomalies in the stratosphere (1987, 1997, 2001, 1994, and 2011). The frequency and duration of blocking patterns in November 2009 were much higher and longer than those in these years. However, not all large negative geopotential height anomalies in the stratosphere and polar vortex migrations were associated with the occurrence of blocking.

From the climatology for 1979–2015, the South American continent is more vulnerable to polar vortex air with low column ozone in spring than Australia and New Zealand. In addition, analysis of the total ozone anomaly around Rio Gallegos in November from the 1979–2015 mean of TOMS/OMI indicates that the negative anomaly in middle and late November 2009 is one of the largest anomalies in magnitude and duration in those 37 years in association with the large negative geopotential height anomaly in the lower stratosphere and the frequent occurrence of blocking patterns.

For a better prediction of the risk of high ultraviolet exposure in late spring at the time of the vortex breakup, not only accurate numerical predictions but also dynamical process studies associated with ozone depletion are needed. Thus, attention should be paid to tropospheric dynamics and climate as well as the polar vortex in the Southern Hemisphere stratosphere.

Acknowledgments

The authors thank K. Kodera and M. Takahashi for useful comments and discussions and Y. Yamashita for performing the REF-C1SD simulation for CCMI. The authors also thank three anonymous reviewers for many useful comments. This research was supported by SATREPS from JST/JICA, the Environment Research and Technology Development Fund from the Ministry of the Environment, Japan (2-1303 and 2-1709), and a grant-in-aid for scientific research from the Ministry of Education, Culture, Sports, Science and Technology (MEXT) of Japan (16H01183 and 16H04052). Chemistry-climate model simulations were performed on NEC-SX9/A (ECO) and NEC-SXACE computers at the Center for Global Environmental Research (CGER), National Institute for Environmental Studies (NIES). ERA-Interim reanalysis data are available at <http://apps.ecmwf.int/datasets/>. Total ozone data of TOMS and OMI are available at https://disc.gsfc.nasa.gov/datasets/TOMSN7L3dtoz_V008/summary?keywords=ozone%20 and https://disc.gsfc.nasa.gov/datasets/TOMSEPL3dtoz_V008/summary?keywords=ozone%20. The REF-C1SD simulation data are stored at the CCMI site of BADC at <http://badc.nerc.ac.uk/browse/badc/wcrp-ccmi/data/CCMI-1/output/NIES>.

References

- Ajtic, J., Connor, B. J., Lawrence, B. N., Bodeker, G. E., Hoppel, K. W., Rosenfield, J. E., & Heuff, D. N. (2004). Dilution of the Antarctic ozone hole into southern midlatitudes, 1998–2000. *Journal of Geophysical Research*, 109, D17107. <https://doi.org/10.1029/2003JD004500>
- Ajtic, J., Connor, B. J., Randall, C. E., Lawrence, B. N., Bodeker, G. E., Rosenfield, J. E., & Heuff, D. N. (2003). Antarctic air over New Zealand following vortex breakdown in 1998. *Annales Geophysicae*, 21(11), 2175–2183. <https://doi.org/10.5194/angeo-21-2175-2003>
- Akiyoshi, H., Nakamura, T., Miyasaka, T., Shiotani, M., & Suzuki, M. (2016). A nudged chemistry-climate model simulation of chemical constituent distribution at northern high-latitude stratosphere observed by SMILES and MLS during the 2009/2010 stratospheric sudden warming. *Journal of Geophysical Research: Atmospheres*, 121, 1361–1380. <https://doi.org/10.1002/2015JD023334>
- Akiyoshi, H., Zhou, L. B., Yamashita, Y., Sakamoto, K., Yoshiki, M., Nagashima, T., et al. (2009). A CCM simulation of the breakup of the Antarctic polar vortex in the years 1980–2004 under the CCMVal scenarios. *Journal of Geophysical Research*, 114, D03103. <https://doi.org/10.1029/2007JD009261>
- Atkinson, R. J., & Plumb, R. A. (1997). Three-dimensional ozone transport during the ozone hole breakup in December 1987. *Journal of Geophysical Research*, 102(D1), 1451–1466. <https://doi.org/10.1029/95JD03756>
- Bancalá, S., Krüger, K., & Giorgetta, M. (2012). The preconditioning of major sudden stratospheric warmings. *Journal of Geophysical Research*, 117, D04101. <https://doi.org/10.1029/2011JD016769>
- Brinksma, E., Ajtic, J., Bergwerff, J. B., Bodeker, G. E., Boyd, I. S., de Haan, J. F., et al. (2002). Five years of observations of ozone profiles over Lauder, New Zealand. *Journal of Geophysical Research*, 107(D14), 4216. <https://doi.org/10.1029/2001JD000737>
- Castanheira, J. M., & Barriopedro, D. (2010). Dynamical connection between tropospheric blockings and stratospheric polar vortex. *Geophysical Research Letters*, 37, L13809. <https://doi.org/10.1029/2010GL043819>
- de Laat, A. T. J., van der A, R. J., Allaart, M. A. F., van Weele, M., Benitez, G. C., Casaccia, C., et al. (2010). Extreme sunbathing: Three weeks of small total O₃ columns and high UV radiation over the southern tip of South America during the 2009 Antarctic O₃ hole season. *Geophysical Research Letters*, 37, L14805. <https://doi.org/10.1029/2010GL043699>
- Dee, D. P., Uppala, S. M., Simmons, A. J., Berrisford, P., Poli, P., Kobayashi, S., et al. (2011). The ERA-Interim reanalysis: Configuration and performance of the data assimilation system. *Quarterly Journal of the Royal Meteorological Society*, 137(656), 553–597. <https://doi.org/10.1002/qj.828>
- Eyring, V., Lamarque, J.-F., Hess, P., Arfeuille, F., Bowman, K., Chipperfield, M. P., et al. (2013). Overview of IGAC/SPARC Chemistry-Climate Model Initiative (CCMI) community simulations in support of upcoming ozone and climate assessments. *SPARC Newsletter*, 40, 48–66.
- Harada, Y., Goto, A., Hasegawa, H., Fujikawa, N., Naoe, H., & Hirooka, T. (2010). A major stratospheric sudden warming event in January 2009. *Journal of the Atmospheric Sciences*, 67(6), 2052–2069. <https://doi.org/10.1175/2009JAS3320.1>
- Harwood, R. S. (1975). The temperature structure of the Southern Hemisphere stratosphere August–October 1971. *Quarterly Journal of the Royal Meteorological Society*, 101, 75–91.
- Iwao, K., & Hirooka, T. (2006). Dynamical quantifications of ozone mini-hole formation in both hemisphere. *Journal of Geophysical Research*, 111, D02104. <https://doi.org/10.1029/2005JD006333>
- Kirchhoff, V. W. J. H., Sahai, Y., Casaccia, C. A. R., Zamorano, B. F., & Valderrama, V. (1997). Observations of the 1995 ozone hole over Punta Arenas, Chile. *Journal of Geophysical Research*, 102, 16,109–16,120.
- Labitzke, K. (1965). On the mutual relation between stratosphere and troposphere during periods of stratospheric warming in winter. *Journal of Applied Meteorology*, 4(1), 91–99. [https://doi.org/10.1175/1520-0450\(1965\)004<0091:OTMRBS>2.0.CO;2](https://doi.org/10.1175/1520-0450(1965)004<0091:OTMRBS>2.0.CO;2)
- Langematz, U., & Kunze, M. (2006). An update on dynamical changes in the Arctic and Antarctic stratospheric polar vortices. *Climate Dynamics*, 27(6), 647–660. <https://doi.org/10.1007/s00382-006-0156-2>
- Martius, O., Polvani, L. M., & Davies, H. C. (2009). Blocking precursors to stratospheric sudden warming events. *Geophysical Research Letters*, 36, L14806. <https://doi.org/10.1029/2009GL038776>
- Mendes, M. C. D., Cavalcanti, I. F. A., & Headies, D. L. (2012). Southern Hemisphere atmospheric blocking diagnostic by ECMWF and NCEP/NCAR data. *Revista Brasileira de Meteorologia*, 27(3), 263–271. <https://doi.org/10.1590/S0102-77862012000300001>
- Mendes, M. C. D., Trigo, R. M., Cavalcanti, I. F. A., & DaCamara, C. C. (2008). Blocking episodes in the Southern Hemisphere: Impact on the climate of adjacent continental areas. *Pure and Applied Geophysics*, 165(9–10), 1941–1962. <https://doi.org/10.1007/s00024-008-0409-4>
- Morgenstern, O., Hegglin, M. I., Rozanov, E., O'Connor, F. M., Abraham, N. L., Akiyoshi, H., et al. (2017). Review of the global models used within phase 1 of the Chemistry-Climate Model Initiative (CCMI). *Geoscientific Model Development*, 10(2), 639–671. <https://doi.org/10.5194/gmd-10-639-2017>
- Mukougawa, H., Hirooka, T., Ichimaru, T., & Kuroda, Y. (2007). Hindcast AGCM experiments on the predictability of stratospheric sudden warming. In A. A. Tsonis & J. B. Elsner (Eds.), *Nonlinear Dynamics in Geosciences* (pp. 221–233). New York: Springer-Verlag. <https://doi.org/10.1007/978-0-387-34918-3>
- Mukougawa, H., Sakai, H., & Hirooka, T. (2005). High sensitivity to the initial condition for the prediction of stratospheric sudden warming. *Geophysical Research Letters*, 32, L17806. <https://doi.org/10.1029/2005GL022909>
- Nash, E. R., Newman, P. A., Rosenfield, J. E., & Schoeberl, M. (1996). An objective determination of the polar vortex using Ertel's potential vorticity. *Journal of Geophysical Research*, 101(D5), 9471–9478. <https://doi.org/10.1029/96JD00066>
- Nishii, K., Nakamura, H., & Orsolini, Y. J. (2011). Geographical dependence observed in blocking high influence on the stratospheric variability through enhancement and suppression of upward planetary-wave propagation. *Journal of Climate*, 24(24), 6408–6423. <https://doi.org/10.1175/JCLI-D-10-05021.1>
- Pérez, A., Crino, E., Aguirre de Cárcer, L., & Jaque, F. (2000). Low-ozone events and three-dimensional transport at midlatitudes of South America during springs of 1996 and 1997. *Journal of Geophysical Research*, 105(D4), 4553–4561. <https://doi.org/10.1029/1999JD901040>
- Plumb, R. A. (1985). On the three-dimensional propagation of stationary waves. *Journal of the Atmospheric Sciences*, 42(3), 217–229. [https://doi.org/10.1175/1520-0469\(1985\)042<0217:OTDPO>2.0.CO;2](https://doi.org/10.1175/1520-0469(1985)042<0217:OTDPO>2.0.CO;2)

- Quiroz, R. S. (1986). The association of stratospheric warmings with tropospheric blocking. *Journal of Geophysical Research*, 91(D4), 5277–5285. <https://doi.org/10.1029/JD091iD04p05277>
- Rees, D., Barnett, J. J., & Labitzke, K. (1990). COSPAR International Reference Atmosphere: 1986. Part II: Middle atmosphere models. *Advances in Space Research*, 10(12). Published for COSPAR by Pergamon Press), 519.
- Sugita, T., Akiyoshi, H., Wolfram, E., Salvador, J., Ohyama, H., & Mizuno, A. (2017). Comparison of ozone profiles from DIAL, MLS, and chemical transport model simulations over Rio Gallegos, Argentina, during the spring Antarctic vortex breakup, 2009. *Atmospheric Measurement Techniques*, 10(12), 4947–4964. <https://doi.org/10.5194/amt-10-4947-2017>
- Taguchi, M. (2008). Is there a statistical connection between stratospheric sudden warming and tropospheric blocking events? *Journal of the Atmospheric Sciences*, 65(4), 1442–1454. <https://doi.org/10.1175/2007JAS2363.1>
- Tibaldi, S., Tosi, E., Navarra, A., & Pedulli, L. (1994). Northern and southern hemisphere seasonal variability of blocking frequency and predictability. *Monthly Weather Review*, 122(9), 1971–2003. [https://doi.org/10.1175/1520-0493\(1994\)122<1971:NASHSV>2.0.CO;2](https://doi.org/10.1175/1520-0493(1994)122<1971:NASHSV>2.0.CO;2)
- Wirth, V. (1993). Quasi-stationary planetary waves in total ozone and their correlation with lower stratospheric temperature. *Journal of Geophysical Research*, 98(D5), 8873–8882. <https://doi.org/10.1029/92JD02820>
- Wolfram, E. A., Salvador, J., Orte, F., D'Elia, R., Godin-Beekmann, S., Kuttippurath, J., et al. (2012). The unusual persistence of an ozone hole over a southern mid-latitude station during the Antarctic spring 2009: A multi-instrument study. *Annales Geophysicae*, 30(10), 1435–1449. <https://doi.org/10.5194/angeo-30-1435-2012>
- Wough, D. W., & Rong, P.-P. (2002). Interannual variability in the decay of lower stratospheric Arctic vortices. *Journal of the Meteorological Society of Japan*, 80(4B), 997–1012. <https://doi.org/10.2151/jmsj.80.997>